

# Enrichment of cholesterol in microdissected Alzheimer's disease senile plaques as assessed by mass spectrometry

Maï Panchal,<sup>\*,†,§</sup> Jacqueline Loeper,<sup>\*\*,§</sup> Jack-Christophe Cossec,<sup>†</sup> Claire Perruchini,<sup>\*,†</sup> Adina Lazar,<sup>\*,†</sup> Denis Pompon,<sup>\*\*,\*</sup> and Charles Duyckaerts<sup>1,\*,†,§</sup>

Laboratoire de Neuropathologie Escourolle,<sup>\*</sup> Hôpital de la Salpêtrière, AP-HP, Paris, France; Centre de Recherche de l'ICM (UPMC, INSERM UMR S 975, CNRS UMR 7225),<sup>†</sup> Paris, France; UPMC Paris Universitatis,<sup>§</sup> Paris, France; Centre de Génétique Moléculaire,<sup>\*\*</sup> Laboratoire d'Ingénierie des Protéines Membranaires, CNRS UPR2167, Gif-sur-Yvette, France

**Abstract** Extensive knowledge of the protein components of the senile plaques, one of the hallmark lesions of Alzheimer's disease, has been acquired over the years, but their lipid composition remains poorly known. Evidence suggests that cholesterol contributes to the pathogenesis of Alzheimer's disease. However, its presence within senile plaques has never been ascertained with analytic methods. Senile plaques were microdissected from sections of the isocortex in three Braak VI Alzheimer's disease cases and compared with a similar number of samples from the adjoining neuropil, free of amyloid- $\beta$  peptide (A $\beta$ ) deposit. Two cases were apoE4/apoE3, and one case was apoE3/apoE3. A known quantity of <sup>13</sup>C-labeled cholesterol was added to the samples as a standard. After hexane extraction, cholesterol content was analyzed by liquid chromatography coupled with electrospray ionization mass spectrometry. The mean concentration of free cholesterol was  $4.25 \pm 0.1$  attomoles/ $\mu\text{m}^3$  in the senile plaques and  $2.2 \pm 0.49$  attomoles/ $\mu\text{m}^3$  in the neuropil ( $t = 4.41$ ,  $P < 0.0009$ ). The quantity of free cholesterol per senile plaque ( $67 \pm 16$  femtomol) is similar to the published quantity of A $\beta$  peptide. The highly significant increase in the cholesterol concentration, associated with the increased risk of Alzheimer's disease linked to the apoE4 allele, suggests new pathogenetic mechanisms.—Panchal, M., J. Loeper, J.-C. Cossec, C. Perruchini, A. Lazar, D. Pompon, and C. Duyckaerts. **Enrichment of cholesterol in microdissected Alzheimer's disease senile plaques as assessed by mass spectrometry.** *J. Lipid Res.* 2010. 51: 598–605.

**Supplementary key words** sterol • brain tissue • neurodegeneration • apolipoprotein E • lipoprotein receptor-related protein • quantitative liquid chromatography coupled with mass spectrometry

Neurofibrillary tangles, mainly composed of hyperphosphorylated tau protein, and senile plaques (SPs) are the two hallmark lesions of Alzheimer's disease (AD) (1–4).

This work was supported by grant Agence Nationale de la Recherche ChoAD. The postdoctoral position of M.P. was funded by the National Alzheimer Plan 2008–2012 (France).

Manuscript received 3 September 2009 and in revised form 18 September 2009.

Published, JLR Papers in Press, September 18, 2009  
DOI 10.1194/jlr.M001859

The core of the SP is made of aggregated amyloid- $\beta$  (A $\beta$ ) peptide. A $\beta$  peptide is cleaved from a type 1 transmembrane protein, the amyloid protein precursor (APP), by the sequential activities of the  $\beta$  and  $\gamma$  secretases. Special staining of microscopic sections from brain samples of AD patients has long suggested that SPs were enriched in lipids (5). The presence of cholesterol among those lipids is plausible since apolipoprotein E (apoE), a transporter of cholesterol, has been found in the SPs by immunohistochemistry (6, 7). The apoE4 allele is currently considered as the risk factor best associated with AD (8). Although the role of cholesterol has remained elusive, a much debated meta-analysis has shown that the use of statins, which inhibit cholesterol synthesis, was associated with a decreased prevalence of AD (9, 10). In cell cultures, the interaction between APP and cholesterol metabolism has been found so intricate that APP has been considered a sensor modulating the cholesterol content of the cell membrane (11).

Histological studies have apparently confirmed the cholesterol enrichment of the SPs in transgenic mice and AD patients (12). Two methods have been used. 1) Filipin, a well-known fluorescent probe of membrane cholesterol, labels the SPs and subsequently resists the photobleaching that rapidly decreases the fluorescence of the surrounding tissue. 2) An enzymatic technique based upon cholesterol oxidase activity was initially devised (and commercialized) for colorimetric cholesterol assay (not for histochemistry). It is based on the oxidation of Amplex Red<sup>®</sup> (10-acetyl-3,7-dihydroxyphenoxazine) into brightly fluorescent resorufin.

Abbreviations: A $\beta$ , amyloid- $\beta$  peptide; AD, Alzheimer's disease; apoE, apolipoprotein E; APP, amyloid protein precursor; LCM, laser capture microdissection; LC-MS, liquid chromatography coupled with mass spectrometry; LRP, low density lipoprotein receptor-related protein; SP, senile plaque.

<sup>1</sup>To whom correspondence should be addressed.  
e-mail: charles.duyckaerts@psl.aphp.fr

Copyright © 2010 by the American Society for Biochemistry and Molecular Biology, Inc.

This article is available online at <http://www.jlr.org>

Both techniques stained the SPs (12, 13). However, the filipin staining was not abolished by cholesterol extraction; the SPs were still stained in the absence of cholesterol oxidase, and resorufin alone was found to stain amyloid. The belief that cholesterol was abundant in the SPs could thus have been based on false positive labeling (14). A more analytical approach was needed. The mere comparison of tissue homogenates from control and AD cases would have been unsatisfactory: tissues contain many structures, such as vessels, cell membranes, or various lesions, that could influence the results and obscure alterations directly linked to the SPs. Another strategy was chosen here: the SPs were microdissected from the rest of the tissue by laser capture microdissection (LCM) and compared with an equivalent volume of surrounding A $\beta$ -free neuropil. The hexane extracts of the microdissected samples were analyzed by liquid chromatography coupled with mass spectrometry (LC-MS). A known amount of [3,4-<sup>13</sup>C] cholesterol was added as an internal standard to quantify the free cholesterol content in SPs and neuropil.

## METHODS

### Cases

AD patients had been enrolled in a brain donation program of the Brain Bank "GIE NeuroCEB" run by a consortium of Patients Associations (including France Alzheimer Association) and declared to the Ministry of Research and Universities, as requested by French Law. An explicit consent had been signed by the patient himself, or by the next of kin, in the name of the patient, in accordance with the French Bioethical Laws. The project had been approved by the ad hoc committee of the Brain Bank. At the time of death, the corpse was transported to the mortuary of a University Hospital belonging to the NeuroCEB network and the brain was removed. One hemisphere, randomly left or right, was fixed in buffered 4% formaldehyde for the neuropathological diagnosis of AD. The other hemisphere was immediately sliced. Samples from the superior temporal gyrus (Brodmann area 22), around 4 cm<sup>3</sup> in volume, were mounted on a cork piece with Cryomount embedding medium and dipped in isopentane cooled by liquid nitrogen. The samples were kept in a deep freezer at -80°C.

### ApoE genotyping

Genomic DNA was extracted from another frozen brain sample. Between 100 and 200  $\mu$ g of brain tissue was minced and homogenized in 2 ml of PBS, pH 7.4. Two milliliters of lysis buffer (100 mM Tris, pH 7.5, 20 mM NaCl, 100 mM EDTA, and 2% SDS) was added, with 80  $\mu$ l of a 400  $\mu$ g/ml proteinase K. The solution was left at 50°C for the night. One volume of a solution of phenol/chloroform/isoamyl alcohol (25:24:1) was added. The sample was mixed for 15 min in an orbital agitator and centrifuged for 10 min at 4,000 rpm. The organic phase was discarded and the process was repeated once on the aqueous phase. A solution of ammonium acetate 10 M, a third of the volume (around 1.33 ml), was added to the aqueous solution and then two volumes (around 10.66 ml) of 96% ethanol at -20°C. After mixing, the precipitated DNA was rinsed twice in 70% ethanol and left to dry. It was resuspended in 100  $\mu$ l of Tris EDTA 10:1.

PCR was performed with the following primers: APOE sense, 5'-TAAGCTTGGCACGGCTGTCCAAGGA-3'; APOE antisense, 5'-ACAGAATTCGCCCCGGCCTGGTACAC-3'. For each sample,

the reaction mixture (50  $\mu$ l) contained 100 ng of human genomic DNA, PCR buffer (1 $\times$ ), 2  $\mu$ l dNTPs (10 mM), 1.5  $\mu$ l forward and reverse primers (10  $\mu$ M), and 0.5  $\mu$ l Taq DNA polymerase (Qiagen, Courtaboeuf, France). The cycling program was carried out after a preheating step at 95°C for 15 min and 35 cycles of denaturation at 95°C for 1 min, annealing at 60°C for 1 min, and extension at 70°C for 2 min in a DNA thermal cycler (AnalyticJena®; Jena, Germany). After purification, 1.5  $\mu$ l of DNA were used in the sequencing reactions (BigDye Terminator® cycle sequencing kit; Applied Biosystems, Villebon sur Yvette, France) using the same primers (see above). The 227 amplified fragments were then purified by Sephadex G-50 resin (Sigma-Aldrich, Saint-Quentin Fallavier, France) and sequenced using the 3730 DNA analyzer (Applied Biosystems).

### Diagnosis

Multiple samples from the formalin-fixed hemisphere, including the hippocampus and isocortical area Brodmann 22, were embedded in paraffin and cut at 5  $\mu$ m of thickness. The sections were stained with hematoxylin-eosin and immunostained with anti-A $\beta$  (6F/3D clone; Dako, Trappes France) and anti-tau (polyclonal rabbit anti-tau antibody; Dako; Trappes code number A 0024). The lesions were staged according to Braak and Braak (15). The density of the SPs was evaluated according to the CERAD protocol (16). The diagnosis criteria of the NIA-Reagan Institute were used (17). Care was taken to select cases with a high number of mature SPs containing an amyloid central core of A $\beta$  peptide. Three sporadic cases, numbers 1, 2, and 3 (ages 64, 78, and 83), at Braak stage VI with "frequent" SPs and NIA-Reagan "high probability" were chosen.

### Samples for microdissection

Ten micrometer thick brain sections from the temporal cortex were obtained from the frozen block with a Leica CM 3050 S cryostat. They were mounted on polyethylene-naphthalate membrane-coated glass slides (P.A.L.M. MembraneSlides 1.0 PEN; Zeiss, Bernried, Germany) and stored until immunostaining at -80°C.

### Immunohistochemistry preceding the microdissection

A method for reliably staining the SPs in the frozen section was needed to enable the observer to clearly identify the areas to be microdissected. The criteria of choice for such a method were as follows: good sensitivity, absence of interference with mass spectrometry, and ease of use. Our observation agreed with the statement of Rufenacht et al. (18): Whereas "amyloid plaques from mouse tissue showed a virtually identical staining with Congo red, thioflavin, or anti-A $\beta$  antibodies,...most plaques from human tissue were reliably detected only by immunostaining." Immunohistochemistry had distinct advantages for our project: SPs are readily identified, and the antibodies being excluded from the hexane during sterol extraction do not interfere with the analysis. Peroxidase-based amplification requires the use of hydrogen peroxide that could alter the lipids. This is why alkaline phosphatase and a chromogen of the Fast Red type were chosen. Detergents and pretreatment, possibly altering the concentration or the structure of cholesterol, were avoided. We were able to visualize the SPs using a rapid immunohistochemistry technique without pretreatment. The frozen brain sections were thawed for a few minutes at room temperature and incubated for 30 min at room temperature in a 200  $\mu$ l solution containing 5  $\mu$ g/ml of monoclonal 6F/3D antibody (specific for the A $\beta$  peptide epitope amino acids 8-17). The samples were then washed three times for 5 min with TBS. Secondary biotinylated goat anti-mouse antibodies (incubated for 15 min at room temperature) were

detected by the biotin-streptavidin-alkaline phosphatase complex using the Dako REAL™ detection system and the alkaline phosphatase/RED kit (Dako; code K5005). The slides were then washed once for 5 min with TBS and once with double distilled water and air-dried. Immunostained mature SPs had a central, highly compact core, separated from a less immunoreactive corona by a clear halo. LCM was performed the same day as immunohistochemistry.

### Microdissection of SPs

The UV laser-based PALM® Microbeam 3.0 (Carl Zeiss, P.A.L.M. Microlaser Technologies, Bernried, Germany) was used to microdissect SPs and Aβ free neuropil. This system resorts to a pulsed 336 nm UV laser beam that is able to cut the section at the focus point but causes minimal damage to the surrounding tissue even at a short distance of the cut (Fig. 1). A final laser pulse produces enough pressure to catapult the microdissected sample into an appropriate collection vial (19). The surface area of the microdissected spot was recorded by the system. Since the thickness of the section was constant (10 μm), the volume of microdissected material could be evaluated by summing the area of the individual spots and multiplying the result by 10 μm.

The laser power was set at 64–84 mW. The laser pulse lasted 1 ms; the spot size was 1 μm. A total of 3,714 SPs were microdissected from three sections per case in three AD cases and collected in the lid of an AdhesiveCap (P.A.L.M. Microlaser Technologies). A similar number of spots, each covering an area comparable to the area occupied by a SP, were captured in the surrounding neuropil, free from Aβ deposit. These control samples were collected in another AdhesiveCap. Finally, each AdhesiveCap contained about 400 plaques or Aβ free neuropil spots of equivalent volume collected from one single microscopic slide. Eighteen AdhesiveCaps were analyzed (three caps for the SPs and three for the Aβ free neuropil = six caps per case in three cases).

### Cholesterol extraction and quantification

**Material.** [3,4-<sup>13</sup>C]cholesterol (99% of the carbon atoms located in positions 3 and 4 are of the <sup>13</sup>C isotope) was obtained from Cambridge Isotope Laboratories. The 99% pure natural cholesterol (“natural cholesterol”), acetonitrile, formic acid, and *n*-hexane (=hexane) were from Sigma-Aldrich and Tris, NaCl, and HCl from VWR (Fontenay-sous-Bois, France). Stock solutions of cholesterol and [3,4-<sup>13</sup>C]cholesterol were prepared at 10 ng/μl solution in ethanol. All solvents used were of analytical grade.

**Methods.** In order to quantify cholesterol in the samples, an internal standard made of 20 ng (51.5 pmol) of [3,4-<sup>13</sup>C]cholesterol was added to the collected material. For each cap, four successive extractions were carried out with 200 μl of hexane. Samples were vortexed and incubated for a few minutes at room temperature, before centrifugation (12,000 rpm, 3 min). The supernatants were pooled in a glass tube. Hexane was evaporated under air flow, and the residue was dissolved in 90 μl acetonitrile.

### LC-MS

The extracts were analyzed by LC-MS. Thirty microliters of the acetonitrile extracts were loaded onto a XTerra® RP C<sub>18</sub> 3.5 μm pore size 4.6 × 10 mm column (Waters, France) and eluted at 55°C with a water:acetonitrile gradient (linear from 80:20 to 25:75 by volume in 5 min and then linear to 0:100 by volume in 15 min, and a final hold of 1 min). Formic acid (0.03% by volume) was included in both solvents to facilitate ionization. The flow rate was 1.3 ml/min. The MS detection was performed using a Micromass ZQ single quadrupole (Waters). Electrospray positive ionization was performed using capillary voltage of 3.5 kV, cone voltage of 30 V, desolvation nitrogen flow of 400 l/h, desolvation temperature of 350°C, and source temperature of 120°C. The MH<sup>+</sup> ions of natural and <sup>13</sup>C labeled cholesterols were detected at *m/z* = 369.3 and 371.3, respectively.

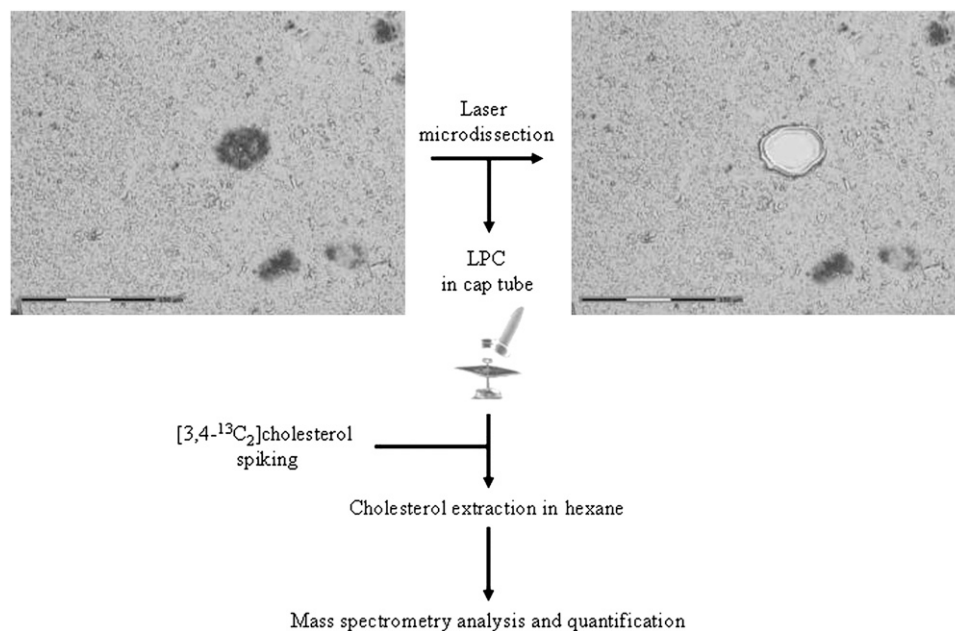


**Fig. 1.** Analytical procedure. The tissue sections were immunostained with the 6F/3D anti-Aβ antibody. SPs were microdissected and catapulted in a cap by laser pressure catapulting (LPC). The samples were spiked with 20 ng of [3,4-<sup>13</sup>C]cholesterol. After sterol extraction with hexane, the preparations were evaporated and dissolved in acetonitrile. MS analysis was performed and quantification was achieved by comparing the ratio of the peak area of natural isotope of free cholesterol with the added [3,4-<sup>13</sup>C]cholesterol internal standard.

## Calibration curves

Increasing amounts of natural cholesterol and of [3,4-<sup>13</sup>C] cholesterol standards were injected in the column. After MS, the peak areas (PAs) of the natural isotope and of <sup>13</sup>C cholesterol were evaluated by numerical integration. Regression curves were calculated and a linear model was applied: cholesterol (injected) = a.PA+b.

## RESULTS

### ApoE status of the cases

Cases 1 and 3 were of the apo ε3/ε4 genotype. Case 2 was ε3/ε3.

### Calibration

The curves for natural cholesterol and [3,4-<sup>13</sup>C]cholesterol standards were not statistically different. The data were pooled and the following regression coefficients were found:  $a = 1.46 \cdot 10^{-5}$  and  $b = -5.76$  with  $r = 0.99$  (Fig. 2), which were applied to both natural and [3,4-<sup>13</sup>C]cholesterol. With these parameters, the calibration line explained 98% of the total variance. The regression line crossed the abscissa at a positive value, indicating that, at low values, the signal was noisy. For practical applications, we considered that the lower limit of quantification of our measurement, defined as the lowest concentration of cholesterol obtained with linearity, was 5 ng of cholesterol and the range of measurement was 5 to 50 ng (Fig. 2). The accuracy, calculated as the difference between the mean of the expected value and the mean of assessed value of cholesterol, was  $-0.77$  ng. We concluded that the systematic bias was limited (and mainly concentrated around the low values; Fig. 3). Eighteen injections of 20 ng of [3,4-<sup>13</sup>C] cho-

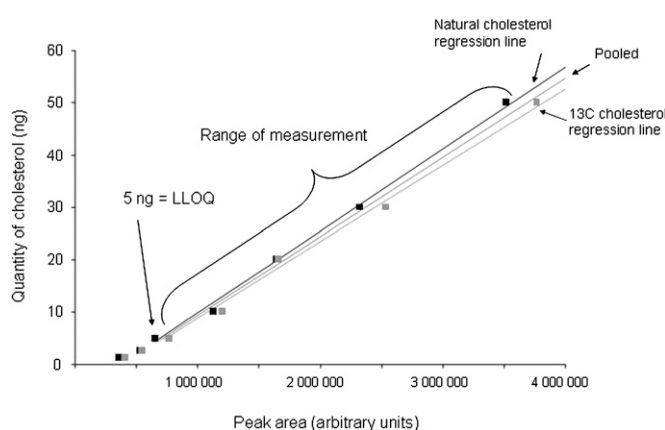


**Fig. 2.** Calibration curves: quantity of cholesterol as a function of the peak areas. Increasing and known amounts of natural cholesterol and of internal [3,4-<sup>13</sup>C]cholesterol standards were extracted and analyzed by LC-MS. The curves obtained with natural and [3,4-<sup>13</sup>C<sub>2</sub>]cholesterol are indicated. Since they were not statistically different, a pooled curve was obtained and used for the subsequent assessment. The parameters of the curve were as follows: quantity of cholesterol =  $1.50 \cdot 10^{-5} \cdot \text{peak area} - 5.68$ . The linear regression explained 98% of the variance. The curve is drawn only in the segment where the measurements were made (see text). LLOQ, lower limit of quantification.

lesterol and multiple assessments of injected natural and [3,4-<sup>13</sup>C] cholesterol standards at 1.25, 2.5, 5, 10, 20, 30, and 50 ng were performed. The mean coefficient of variation between measurements was 7% when the values taken into account were located in the range of quantification. The standard deviation of the measurement (mean = 1.42 ng) was similar for low and high values of cholesterol, suggesting homoscedasticity. Injection of natural cholesterol standard gave rise to about 1% crosstalk on the channel at  $m/z = 371.3$  as expected from the natural <sup>13</sup>C abundance. This signal has not been taken into account in peak integration because of the small values of cholesterol content. In contrast, no signal was detected at the  $m/z$  369.3 when [3,4-<sup>13</sup>C]cholesterol was injected. In each case, only one peak was produced per analyte at the expected retention time of 12.35 min (Fig. 4). We made sure that hexane did not extract contaminants from the AdhesiveCap by analyzing hexane left in an empty cap, following all the steps of the extraction protocol. No MS signal at the expected retention time could be detected above noise at both  $m/z$ .

### Estimation of the quantity of cholesterol in SPs and Aβ free neuropil

Each AdhesiveCap containing microdissected samples was spiked with 51.5 pmol (20 ng) of [3,4-<sup>13</sup>C]cholesterol as internal standard and was independently extracted with hexane. The quantity of measured <sup>13</sup>C standard was estimated with the previously calculated regression coefficients. Since the number and the volume of the microdissected samples had been recorded, the quantity of cholesterol could be expressed either per SP or per  $\mu\text{m}^3$ .

Between 213 and 516 (mean: 412) microdissected SPs and equivalent volumes of neuropil were assessed three times for each of the three cases. The mean concentration of cholesterol was  $4.25 \pm 0.10$  attmol/ $\mu\text{m}^3$  (mean  $\pm$  SE) for the SPs versus  $2.20 \pm 0.49$  attmol/ $\mu\text{m}^3$  for the neuropil. An ANOVA was performed taking into account the “case” and the “SP/ neuropil” factors (Fig. 5). The power of the test was 0.99 attmol/ $\mu\text{m}^3$  for the difference between SP and neuropil and 0.21 attmol/ $\mu\text{m}^3$  for the difference between cases. The mean difference between SP and neuropil was  $2.04$  attmol/ $\mu\text{m}^3$  (ddl = 1,  $F = 19.45$ ,  $t = 4.41$ , and  $P < 0.0009$ ). The mean difference between the cases was not significant for any pair of cases. There was no interaction between the “cases” and “SP/neuropil” factors. The quantity of cholesterol per SP was calculated by dividing the total quantity of free cholesterol by the number of microdissected SPs. We found an average of  $67 \pm 16$  fmol (mean  $\pm$  SE) of free cholesterol per plaque.

## DISCUSSION

Using LCM on cryostat sections of Brodmann area 22, immunostained for Aβ peptide, we microdissected cored SPs and Aβ free adjoining neuropil. The presence of free cholesterol was evaluated in the two types of samples by LC-MS. The addition of a known quantity of a [3,4-<sup>13</sup>C] cholesterol standard made the quantitative assessment

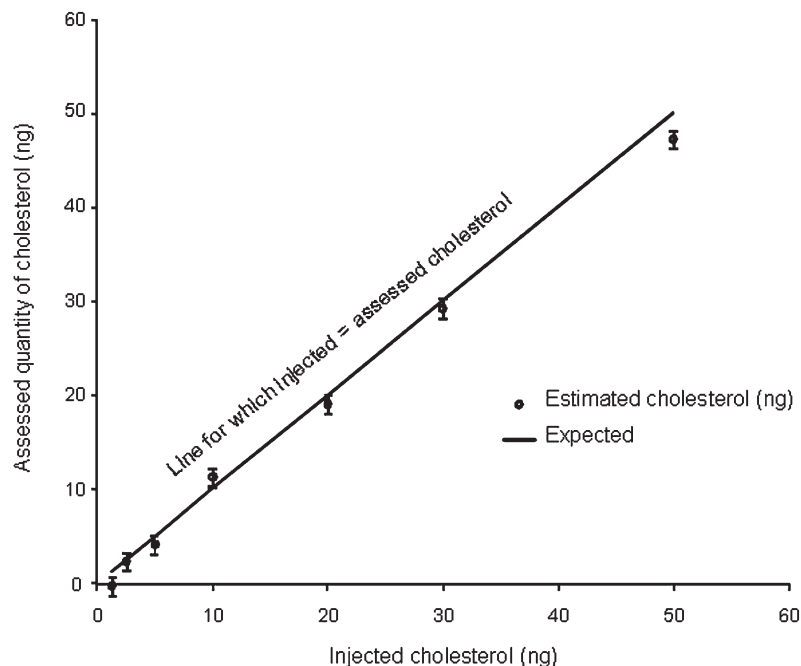


**Fig. 3.** Precision and accuracy. The quantities of assessed cholesterol are plotted against the known quantities of cholesterol injected into the column. A line of slope 1, representing the theoretical line for which estimated quantity = injected quantity, is drawn to show deviation from the theoretical value. The bars are 1 SD above and below the mean estimates.

possible. Free cholesterol, using the same stable isotope as internal standard, has already been assessed in subcellular membranes of Chinese hamster ovary cells (20). To our knowledge, our report describes, for the first time, the quantification of free cholesterol content in microdissected samples. It is also the first report that analyzes a lipid component in microdissected SPs from human AD brain tissue. We found that the SPs were greatly enriched in free cholesterol. The concentration of cholesterol could reach twice the value of cholesterol that was found in the A $\beta$  free neuropil. This is all the more surprising that microdissected neuropil was probably contaminated by

SPs since, if it easy to identify immunopositive spots, it is impossible to make sure that apparently A $\beta$ -free spots do not include a partial volume of a nearby SP. This is why the cholesterol enrichment may actually be even higher. The question of the presence of cholesterol in the so-called diffuse deposits, which are large immunoreactive areas found in AD patients as well as in cognitively normal individuals (21), has not been solved by this experiment, focused on mature SPs. It should be investigated with other strategies allowing more sensitive immunohistochemical detection of A $\beta$  peptide and involving other areas (such as the cerebellum where diffuse deposits are largely predominant).

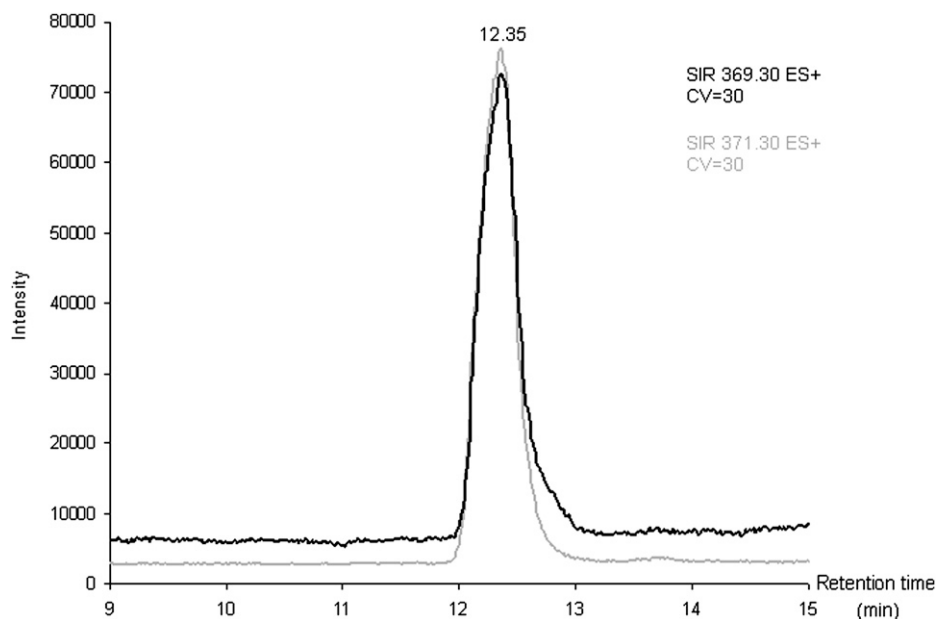


**Fig. 4.** Example of a chromatogram single ion recording (SIR) chromatogram of 20 ng of extracted cholesterol (at  $m/z$  369.3) and [3,4- $^{13}\text{C}_2$ ]cholesterol standards (at  $m/z$  371.3).

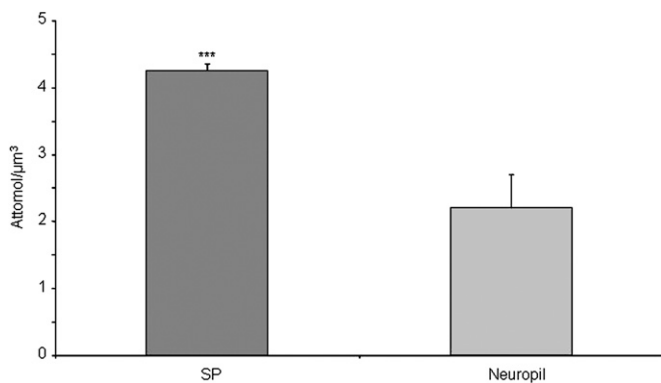


**Fig. 5.** Quantification of free cholesterol content in the neuropil and in SPs. Samples from three different human AD brains were used, and three measurements were performed on each case. Cholesterol concentration per microdissected volume is given in attomol/ $\mu\text{m}^3$ . Bars = 1 SE of the mean for three measurements. The ANOVA indicated no difference between the cases and a mean difference of 2.04 attomol/ $\mu\text{m}^3$  between SP and A $\beta$  free neuropil (ddl = 1, F = 19.45, t = 4.41, and  $P < 0.0009$ ).

Evidence for the presence of cholesterol in the SPs has already been presented (12, 13). However, the histochemical cholesterol oxidase method that was used on tissue sections was proven to be unreliable; on the other hand, the cholesterol probe filipin could have labeled the SPs unspecifically (14). Our alternative approach using LCM and LC-MS avoids these drawbacks and additionally allows a quantitative measurement.

Cholesterol that we detected in the SP was free as it is in cellular membranes. The presence of apoE in the SP is probably related to this accumulation of free cholesterol. ApoE plays an important role in the transport of cholesterol. Immunohistochemistry has shown its presence in cored SPs (6). This neuropathological finding has preceded the discovery that the  $\epsilon 4$  allele of the apoE gene was an important risk factor of AD (8) and has been confirmed several times since (7, 22). The number of cases was evidently too small to permit the study of the influence of the apoE genotype on cholesterol concentration. Two cases had one apo $\epsilon 4$  allele. In the first one, the difference in cholesterol concentration between neuropil and SPs was the largest; in the second apo $\epsilon 4$ /apo $\epsilon 3$  case, it was the smallest, suggesting at least that the apoE genotype is not the only determinant of the cholesterol concentration. However, since the cholesterol efflux from neurons depends on the apoE isoform (E2 > E3 > E4) (23), it is probable that the content of the SPs in apoE and cholesterol will vary with the genotype; this point has to be further explored in a larger series of cases. Moreover, a receptor of apoE, the LDL receptor-related protein (LRP), has also been identified by immunohistochemistry around the core of the SP (24). Various ligands of LRP, among which apoE, have been shown to stimulate neuritic outgrowth (25). They could be involved in the formation of the neuritic corona of the SP. Dense cored A $\beta$  plaques spontaneously form in APP(V717F) transgenic mice. When these animals are crossed with apoE knocked-out mice, the deposits of A $\beta$  peptide are only of the diffuse type (26)

and are devoid of LRP immunoreactivity (24). This result suggests that LRP is upregulated in the presence of apoE in the SP and that apoE is necessary to the concentration of A $\beta$  peptide in the core of the plaque. Finally, it has recently been suggested that the SP contains phospholipids (27) that are accumulated in its periphery.

A $\beta$  peptide could be associated, during or just after its secretion, with lipid particles that would permit its extracellular transport. The association could, on the contrary, be secondary, as a reaction to the precipitation of the A $\beta$  fibrils. The chronology of apoE accumulation pleads for the latter hypothesis: it has indeed been observed that apoE immunoreactivity is generally absent from the early, diffuse deposits of A $\beta$  peptide (7), and LRP is not found in apoE negative SPs (24). However, one should keep in mind that the concentration of A $\beta$  peptide and of the molecules that might be associated with it is much lower in diffuse deposits and could remain below the detection limit. Moreover, if the A $\beta$  fibrils were secondarily associated with cholesterol, apoE, and LRP, synthetic A $\beta$  peptide injected in wild-type or APP transgenic mice should also be secondarily associated with the same partners. The injections of synthetic A $\beta$  peptide, however, only resulted in amorphous masses of material. By contrast, the injection of still poorly defined cerebral extracts from patients or APP transgenic mice (28) accelerated the formation of SPs as soon as they contained an increased concentration of A $\beta$  peptide.


On the other hand, the hypothesis that A $\beta$  peptide is embedded in a lipoprotein particle during its secretion, or shortly after, helps to explain why the peptide remains in solution in the extracellular space and can be concentrated in the SP. ApoE has been shown to induce the efflux of cholesterol (23) in lipid particles, isolated from the supernatant of cell culture (29).

The choice between the two scenarios, one in which A $\beta$  peptide is secreted with lipid partners and apoE, and the other, in which fibrillar A $\beta$  structures are secondarily associated with lipids and apoE, largely relies on a better understanding of the content of the SP. Microdissection now provides the technology adapted to reach this goal. The LC-MS method that we used here, necessitated a priori knowledge of the species that was studied to determine which deuterated standard had to be added, in known quantity, to the samples. Further studies, relying on other strategies (electrospray MS-MS and mass spectrometry imaging), have to determine if other membrane lipids are to be found in the amyloid deposit of the SPs. In the MS-MS approach, no a priori hypotheses concerning the accumulated lipids are needed. This technology could help determining whether cholesterol has been oxidized or esterified or whether any of the A $\beta$  peptide is covalently modified by cholesterol as has been suggested (30)

A $\beta$  peptides have a natural tendency to form oligomers that aggregate as fibrils. It is, today, generally admitted that oligomers are the toxic species while fibrils are devoid of effects. Soluble A $\beta$  dimers have been extracted from AD brains and have been shown to potently impair synapse structure and function (31). It has been imagined that

plaque cores could act as reservoirs for inert fibrils and play a protective role. Natural lipids, such as cholesterol, sphingomyelin, and gangliosides, “destabilize and rapidly resolubilize mature A $\beta$  amyloid fibers” in oligomeric toxic aggregates (11, 32). The free cholesterol that we identified in the SPs could thus be noxious by helping the reversion of amyloid fibrils into toxic oligomers.

The amount of A $\beta$  peptide contained in one SP is 50 to 100 fmol as estimated by LC-MS following SP microdissection (18). With  $67 \pm 16$  fmol of cholesterol per SP, we reached the completely unexpected result that there was an equivalent number of A $\beta$  peptide and of free cholesterol molecules per plaque. This mole-to-mole ratio suggests the direct interaction of one molecule of A $\beta$  to one molecule of cholesterol and should prompt new investigations on this possibly physical interaction.

Several recent studies point to the role of cholesterol in the metabolism of APP. APP has even been considered as a “cholesterol sensor” (11). The massive accumulation of cholesterol, at a concentration similar to that of A $\beta$  peptide itself, is a new piece of information that may be crucial in the unraveling of the pathogenesis of AD. 

The authors thank Dr. Dominique Wendum and Sylvie Dumont from technological platform IFR65 (Saint-Antoine Hospital, Paris) for their help in LCM. The skilful technical assistance of Luce Dauphinot and the advice of Marie-Claude Potier are gratefully acknowledged.

## REFERENCES

- Fisher, O. 1907. Miliare Nekrosen mit drusigen Wucherungen der Neurofibrillen, eine regelmässige Veränderung der Hirnrind bei seniler Demenz. *Monatsschr. Psychiatr. Neurol.* **22**: 361–372.
- Duyckaerts, C., B. Delatour, and M. C. Potier. 2009. Classification and basic pathology of Alzheimer disease. *Acta Neuropathol.* **118**: 5–36.
- Duyckaerts, C., and D. Dickson. 2003. Neuropathology of Alzheimer’s disease. In *Neurodegeneration: The Molecular Pathology of Dementia and Movement Disorders*. D. Dickson, editor. ISN Neuropath Press, Basel, Switzerland. 47–65.
- Alzheimer, A. 1907. Über eine eigenartige Erkrankung der Hirnrinde. *Allgemeine Zeitschr Psychiatr Gerichtlich Med.* **64**: 146–148.
- Braunmühl von A. 1957. Handbuch der speziellen pathologischen Anatomie und Histologie. In *Alterserkrankungen des Zentralnervensystems. Senile Involution. Senile Demez. Alzheimersche Krankheit*. F. H. O. Lubarsch and R. Rössle, editors. Springer Verlag, Berlin. 337–539.
- Namba, Y., M. Tomonaga, H. Kawasaki, E. Otomo, and K. Ikeda. 1991. Apolipoprotein E immunoreactivity in cerebral amyloid deposits and neurofibrillary tangles in Alzheimer’s disease and kuru plaque amyloid in Creutzfeldt-Jakob disease. *Brain Res.* **541**: 163–166.
- Uchihara, T., C. Duyckaerts, F. Lazarini, K. Mokhtari, D. Seilhean, P. Amouyel, and J.J. Hauw. 1996. Inconstant apolipoprotein E (ApoE)-like immunoreactivity in amyloid beta protein deposits: relationship with APOE genotype in aging brain and Alzheimer’s disease. *Acta Neuropathol.* **92**: 180–185.
- Strittmatter, W. J., A. M. Saunders, D. Schmechel, M. Pericak-Vance, J. Enghild, G. S. Salvesen, and A. D. Roses. 1993. Apolipoprotein E: high avidity binding to  $\beta$ -amyloid and increased frequency of type 4 allele in late-onset familial Alzheimer disease. *Proc. Natl. Acad. Sci. USA.* **90**: 1977–1981.
- Wolozin, B., W. Kellman, P. Ruosseau, G. G. Celesia, and G. Siegel. 2000. Decreased prevalence of Alzheimer disease associated with 3-hydroxy-3-methylglutaryl coenzyme A reductase inhibitors. *Arch. Neurol.* **57**: 1439–1443.
- Wolozin, B., J. Manger, R. Bryant, J. Cordy, R. C. Green, and A. McKee. 2006. Re-assessing the relationship between cholesterol, statins and Alzheimer’s disease. *Acta Neurol. Scand. Suppl.* **185**: 63–70.
- Beel, A. J., C. K. Mobley, H. J. Kim, F. Tian, A. Hadziselimovic, B. Jap, J. H. Prestegard, and C. R. Sanders. 2008. Structural studies of the transmembrane C-terminal domain of the amyloid precursor protein (APP): does APP function as a cholesterol sensor? *Biochemistry.* **47**: 9428–9446.
- Mori, T., D. Paris, T. Town, A. M. Rojiani, D. L. Sparks, A. Delledonne, F. Crawford, L. I. Abdullah, J. A. Humphrey, D. W. Dickson, et al. 2001. Cholesterol accumulates in senile plaques of Alzheimer disease patients and in transgenic APP(SW) mice. *J. Neuropathol. Exp. Neurol.* **60**: 778–785.
- Burns, M. P., W. J. Noble, V. Olm, K. Gaynor, E. Casey, J. LaFrancois, L. Wang, and K. Duff. 2003. Co-localization of cholesterol, apolipoprotein E and fibrillar Abeta in amyloid plaques. *Brain Res. Mol. Brain Res.* **110**: 119–125.
- Lebouvier, T., C. Perruchini, M. Panchal, M. C. Potier, and C. Duyckaerts. 2009. Cholesterol in the senile plaque: often mentioned, never seen. *Acta Neuropathol.* **117**: 31–34.
- Braak, H., and E. Braak. 1991. Neuropathological staging of Alzheimer-related changes. *Acta Neuropathol.* **82**: 239–259.
- Mirra, S. S., A. Heyman, D. McKeel, S. M. Sumi, B. J. Crain, L. M. Brownlee, F. S. Vogel, J. P. Hughes, G. van Belle, and L. Berg. 1991. The consortium to establish a registry for Alzheimer’s disease (CERAD). Part II. Standardization of the neuropathological assessment of Alzheimer’s disease. *Neurology.* **41**: 479–486.
- National Institute on Aging and Reagan Institute Working Group on Diagnostic Criteria. 1997. Consensus recommendations for the postmortem diagnosis of Alzheimer’s disease. *Neurobiol. Aging.* **18**: S1–S2.
- Rüfenacht, P., A. Guntert, B. Bohrmann, A. Ducret, and H. Dobeli. 2005. Quantification of the A beta peptide in Alzheimer’s plaques by laser dissection microscopy combined with mass spectrometry. *J. Mass Spectrom.* **40**: 193–201.
- Schutze, K., Y. Niyaz, M. Stich, and A. Buchstaller. 2007. Noncontact laser microdissection and catapulting for pure sample capture. *Methods Cell Biol.* **82**: 649–673.
- Sandhoff, R., B. Brugger, D. Jeckel, W. D. Lehmann, and F. T. Wieland. 1999. Determination of cholesterol at the low picomole level by nano-electrospray ionization tandem mass spectrometry. *J. Lipid Res.* **40**: 126–132.
- Delaère, P., C. Duyckaerts, C. Masters, K. Beyreuther, F. Piette, and J. Hauw. 1990. Large amounts of neocortical beta A4 deposits without neuritic plaques nor tangles in a psychometrically assessed, non-demented person. *Neurosci. Lett.* **116**: 87–93.
- Cho, H. S., B. T. Hyman, S. M. Greenberg, and G. W. Rebeck. 2001. Quantitation of apoE domains in Alzheimer disease brain suggests a role for apoE in Abeta aggregation. *J. Neuropathol. Exp. Neurol.* **60**: 342–349.
- Michikawa, M., Q. Fan, I. Isobe, and K. Yanagisawa. 2000. Apolipoprotein E exhibits isoform-specific promotion of lipid efflux from astrocytes and neurons in culture. *J. Neurochem.* **74**: 1008–1016.
- Arelin, K., A. Kinoshita, C. M. Whelan, M. C. Irizarry, G. W. Rebeck, D. K. Strickland, and B. T. Hyman. 2002. LRP and senile plaques in Alzheimer’s disease: colocalization with apolipoprotein E and with activated astrocytes. *Brain Res. Mol. Brain Res.* **104**: 38–46.
- Qiu, Z., B. Hyman, and G. Rebeck. 2004. Apolipoprotein E receptors mediate neurite outgrowth through activation of p44/42 mitogen-activated protein kinase in primary neurons. *J. Biol. Chem.* **279**: 34948–34956.
- Irizarry, M. C., B. S. Cheung, G. W. Rebeck, S. M. Paul, K. R. Bales, and B. T. Hyman. 2000. Apolipoprotein E affects the amount, form, and anatomical distribution of amyloid beta-peptide deposition in homozygous APP(V717F) transgenic mice. *Acta Neuropathol.* **100**: 451–458.
- Rak, M., M. Del Bigio, S. Mai, D. Westaway, and K. Gough. 2007. Dense-core and diffuse Abeta plaques in TgCRND8 mice studied with synchrotron FTIR microspectroscopy. *Biopolymers.* **87**: 207–217.
- Meyer-Luehmann, M., J. Coomaraswamy, T. Bolmont, S. Kaeser, C. Schaefer, E. Kilger, A. Neuenschwander, D. Abramowski, P. Frey, A. L. Jaton, et al. 2006. Exogenous induction of cerebral beta-amyloidogenesis is governed by agent and host. *Science.* **313**: 1781–1784.
- Michikawa, M., J. S. Gong, Q. W. Fan, N. Sawamura, and K. Yanagisawa. 2001. A novel action of alzheimer’s amyloid beta-protein

(Abeta): oligomeric Abeta promotes lipid release. *J. Neurosci.* **21**: 7226–7235.

30. Bieschke, J., Q. Zhang, E. Powers, R. Lerner, and J. Kelly. 2005. Oxidative metabolites accelerate Alzheimer's amyloidogenesis by a two-step mechanism, eliminating the requirement for nucleation. *Biochemistry.* **44**: 4977–4983.
31. Shankar, G. M., S. Li, T. H. Mehta, A. Garcia-Munoz, N. E. Shepardson, I. Smith, F. M. Brett, M. A. Farrell, M. J. Rowan, C. A. Lemere, et al. 2008. Amyloid-beta protein dimers isolated directly from Alzheimer's brains impair synaptic plasticity and memory. *Nat. Med.* **14**: 837–842.
32. Martins, I. C., I. Kuperstein, H. Wilkinson, E. Maes, M. Vanbrabant, W. Jonckheere, P. Van Gelder, D. Hartmann, R. D'Hooge, B. De Strooper, et al. 2008. Lipids revert inert Abeta amyloid fibrils to neurotoxic protofibrils that affect learning in mice. *EMBO J.* **27**: 224–233.